Food Innovation and Advances

ARTICLE

Open Access

https://doi.org/10.48130/fia-0026-0011

Food Innovation and Advances **2026**, 5(1): 133–144

A biodegradable film based on sodium alginate–gelatin involving a mulberry anthocyanin extract for fish oil packaging

Yawen Lv[1], Jingjing Yang[1], Ting Luo[2] and Hongmei Liao[1*]

[1] *School of Food Science and Technology, Jiangnan University, 1800 Lihu Avenue, Wuxi, Jiangsu 214122, China*
[2] *Department of Food Science, University of Otago, 90 Union Place East, Dunedin 9054, New Zealand*
* Correspondence: hmeiliao@jiangnan.edu.cn (Liao H)

Abstract

Driven by the 'dual carbon' strategy and the imperative of a circular economy, food packaging is undergoing a ternary upgrade. In this study, mulberry anthocyanin extract (MAE) was upcycled into a natural, dual-function active principle that concurrently delivers antioxidant capacity and ultraviolet (UV) barrier activity. It was incorporated with an edible sodium alginate–gelatin (SG) based film to engineer a next-generation biodegradable antioxidant film. The dose-dependent impacts of MAE on the film's mechanical signature, radical-scavenging efficacy, optical performance, and practical utility in fish oil packaging were systematically examined. MAE obtained from a residue of mulberry juice fermentation had 296.86 mg/g total polyphenols and 146.50 mg/g anthocyanins, primarily cyanidin-3-glucoside and cyanidin-3-rutinoside. When 0.2 mg/mL MAE (SG-2MAE) was added, the tensile strength of SG films increased from 48.33 to 50.98 MPa. When 0.4 mg/mL MAE was incorporated, the antioxidant activity of SG-4MAE film against 2,2'-biazido-bis-3-ethyl-benzothiazoline-6-sulfonic acid (ABTS) increased by 158%, whereas transmittance (600 nm) decreased by 33.7%, indicating enhanced UV blocking. When applied for packaging fish oil, the SG-MAE film delayed oxidation better than the unpackaged sample after 4 weeks' storage by directly blocking oxygen, releasing antioxidant constituents, and adsorbing residual oxygen. In summary, SG-MAE films showed excellent comprehensive properties and high antioxidant properties, and could be used as active packaging materials for fish oil.

Citation: Lv Y, Yang J, Luo T, Liao H. 2026. A biodegradable film based on sodium alginate–gelatin involving a mulberry anthocyanin extract for fish oil packaging. *Food Innovation and Advances* 5(1): 133–144 https://doi.org/10.48130/fia-0026-0011

Introduction

Traditional packaging materials, such as polyethylene, polypropylene, and metal-based packaging, have caused environmental pollution problems because of their nonbiodegradability and potential toxicity. As consumers become more aware of sustainability and environmental issues, it is urgent to develop biodegradable and edible films using natural biopolymers. Sodium alginate, a naturally occurring polysaccharide extracted from brown seaweed, is widely recognized for its excellent film-forming properties, biodegradability, and nontoxic nature[1]. When gelatin is mixed with sodium alginate, the film's tensile strength, elongation at break, and physical qualities improve, allowing it to handle stringent food packaging standards. It has reported that sodium alginate and gelatin can be used as packaging materials for soybean. Gelatin, a protein derived from collagen, is commonly used in food packaging because of its ability to enhance biopolymeric films' mechanical properties, flexibility, and thermal stability[2]. Biodegradable films composed of gelatin exhibit good mechanical properties; however, these films still have some limitations. Packaging films based on gelatin may dissolve, swell, or decompose upon contact with moisture[3]. It has been shown that the hardness of gelatin increases linearly with an increase in gelatin concentration, and gelatin below its melting temperature (37–40 °C) exhibits cold solidification, which is unfavorable for consumption[4]. However, compounding gelatin with other biodegradable packaging materials can significantly improve its moisture resistance, elasticity, flexibility, and stiffness[5]. In addition, our previous study found that films prepared with a sodium alginate to gelatin ratio of 7:3 has excellent mechanical properties and good barrier properties, and the addition of rose polyphenols effectively delayed the oxidation of edible oils.

Natural antioxidants have become an important trend in the the future development of foods. Introducing natural antioxidants such as polyphenols (phenolic acids, flavonoids, anthocyanins, lignans, and stilbenes), carotenoids (lutein and carotene), and vitamins (vitamins E and C) into packaging films can further enhance their functional properties[6]. Anthocyanins are water-soluble flavonoid pigments found readily available in various fruits and vegetables, with free radical scavenging and antioxidant activities[7]. Anthocyanins shows strong antioxidant activity and act as antioxidants by interrupting the oxidation reaction chain. Films with anthocyanins inhibit photo-oxidation by improving the optical barrier property. One study has been carried out on a functional edible film of olive oil[8]. Mulberry pomace, the residue product of processed materials, is rich in anthocyanins and can be used as an anthocyanin source[9].

Fish oil is usually stored at low temperatures, away from light, and in airtight containers. It has abundant omega-3 polyunsaturated fatty acids (PUFAs), which are known to have positive health effects especially in preventing inflammatory, neurological, and cardiovascular diseases[10]. However, PUFAs' susceptibility to oxidative degradation remains a significant challenge in developing and preserving fish oil-based products[11]. The oxidation of unsaturated fatty acids leads to rancid odors, reduced nutritional value, and the generation of potentially harmful oxidation products such as aldehydes and hydroperoxides. Therefore, ensuring the oxidative stability of fish oils is essential to maintain their quality, functionality, and shelf life throughout storage and distribution. It has suggested that we could use natural antioxidants like gallic acid to prevent oxidation[12] or to scavenge peroxide radicals formed at the start of the oxidation reaction before the chain reaction[13]. A novel fish oil package may be a potential choice. However, few studies have used a biodegradable film for packaging fish oil. Therefore, we prepared a film with light

© The Author(s)

barrier and antioxidant properties for packaging fish oil based on sodium alginate and gelatin with mulberry anthocyanins.

This study aimed to prepare a novel biodegradable packaging film with sodium alginate and gelatin (SG), incorporating a mulberry anthocyanin extract (MAE) to act as an antioxidant and provide light-blocking properties. The primary objectives were to evaluate the potential application of SG-MAE films in packaging fish oil, thus offering a sustainable and efficient alternative to conventional packaging materials. The incorporation of MAE into the SG film matrix not only imparts antioxidant ability but also contributes to the film's ability to act as a light barrier. This dual functionality is crucial for protecting fish oil, which is highly susceptible to oxidation when exposed to light. It is expected to provide valuable insights into the development of active packaging materials that can effectively protect light-sensitive foods such as fish oil. The findings will highlight the potential of using natural antioxidants and light-blocking agents in biodegradable films, thereby offering a more sustainable and functional packaging solution.

Materials and methods

Materials

Hydrochloric acid, methanol, ethanol, and gelatin were purchased from Sinopharm Chemical Reagent Co., Ltd. (Shanghai, China). Chemicals such as 1,1-diphenyl-2-trinitrophenylhydrazine (DPPH), 2,2'-biazido-bis-3-ethylbenzothiazoline-6-sulfonic acid (ABTS), copper sulfate, sodium alginate, and fish oil (18% eicosapentaenoic acid, 20% omega-3 PUFAs) were purchased from Shanghai Macklin Biochemical Technology Co., Ltd. (Shanghai, China). Mulberry pomace was obtained from a local fruit wine fermentation enterprise in Wuxi City.

Extraction and purification of anthocyanins from mulberry pomace

MAE was extracted and purified according to Ai et al.[14] with slight modifications. Specifically, mulberry pomace was mixed with a 60% ethanol aqueous solution (v/v, pH = 4) at a solid–liquid ratio of 1:10, and the mixture was stirred at 40 °C for 1 h under dark conditions. Then the mixture was centrifuged at 7,552 × g for 10 min, and the suspension was concentrated using an evaporator (RV8, Eka, Staufen, Germany) at 40 °C under atmospheric pressure. The residue was the crude anthocyanin extract, which was stored at −20 °C for further purification over the next 7 d.

The crude extract was first passed through an AB-8 macroporous resins column (50 mm × 400 mm) at a flow rate of 1 mL/min. Then the anthocyanin extract was eluted from the AB-8 macroporous resin with 70% ethanol containing 0.1% HCl (v/v), at a flow rate of 1 mL/min. The eluant was collected and concentrated by evaporation. Finally, the eluant was freeze-dried with a lyophilizer (DC801, Yamato Scientific Co., Ltd., Japan) and stored at −20 °C for further application in the film-forming process.

Characterization of MAE

The total phenolics and anthocyanins

The total phenolic in MAE was determined using the Folin–Ciocalteu assay[15]. In short, a 1 mg/mL MAE solution was prepared with deionized water, then each 1 mL of the MAE solution was mixed with 1 mL Folin–Ciocalteau reagent, 3 mL Na_2CO_3 (7.5%, w/v), and 5 mL distilled water. Then the mixture was incubated at 30 °C for 1 h away from the light, and its absorbance at 760 nm was measured using an ultraviolet (UV) mini-124 spectrophotometer (Shimadzu Corporation, Kyoto, Japan). Total phenolics of the samples are presented as mg of gallic acid equivalents per 1-g sample.

The anthocyanin content was determined using the differential pH method[16]. Briefly, the absorbance at 510 and 700 nm of the MAE solution was measured. The content was expressed as mg cyanidin-3-O-glucoside equivalent/g extract, and was calculated by Eqs (1) and (2) as follows:

$$A = (A_{510} - A_{700})_{pH_{1.0}} - (A_{510} - A_{700})_{pH_{4.5}} \quad (1)$$

$$Total\ anthocyanins\ (mg/g) = \frac{A \times MW \times DF \times V \times 10}{\varepsilon \times L \times M} \quad (2)$$

where, A is the absorbance, MW is the molecular weight of cyanidin-3-O-glucoside (449.2 g/mol), DF is the dilution concentration, V is the volume of extracted solvent (mL), ε is the extinction coefficient of cyanidin-3-O-glucoside (28,000 L/cm/mol), L is the radiant length (cm), and M is the mass of the anthocyanin extract (g).

Main anthocyanins in MAE determined by ultrahigh-performance liquid chromatography–tandem mass spectrometry

The anthocyanins in MAE were analyzed by ultrahigh-performance liquid chromatography–tandem mass spectrometry (UPLC-MS) according to Chen et al.[17]. The MAE samples were dissolved in distilled water to prepare a 1 mg/mL MAE solution and then centrifuged at 5,180 × g for 10 min at 4 °C. The specific detection conditions of UPLC-MS were as follows: a bridged ethylene hybrid (BEH) C18 column (100 × 2.1 mm, 1.7 μm); a diode array detector (DAD) with a detection wavelength at 535 nm; an injection volume of 2 μL. The mobile phase consisted of water (Solvent A) and acetonitrile (Solvent B), each containing 0.1% formic acid. The flow rate was 0.3 mL/min. The column was maintained at 45 °C, and a gradient elution was performed over 10 min. The mass spectrometry (MS) detection parameters were optimized for electrospray Ionization positive mode (ESI+) scanning with a mass range of 20–1,000 m/z. Additional MS conditions included a gas temperature of 400 °C, a gas flow rate of 700 L/h, a collision energy of 25 eV, a cone voltage of 30 V, a nebulizer pressure of 50 psi, and a capillary voltage of 3.5 kV.

Antioxidant activity of MAE

The antioxidant activity of MAE was determined according to a previous study with slight modifications[14]. To determine the DPPH scavenging activity, each 100-μL MAE solution (0.01, 0.05, 0.1, 0.2, 0.4, 0.6, 0.8, and 1.0 mg/mL) was mixed with 4 mL of a DPPH solution (0.14 mmol/L) and reacted for 30 min in the dark. To determine the ABTS scavenging activity, each 100 μL MAE solution (0.01–1.0 mg/mL) was mixed with 3.9 mL of an ABTS solution (consisting of a 1:1 mixture of 7 mmol/L ABTS and 2.45 mmol/L $K_2S_2O_8$) and reacted for 30 min in the dark. Then the absorbance of the mixture at 517 and 734 nm was determined with a spectrophotometer (UV mini-124, Shimadzu Corporation, Kyoto, Japan) for calculating the free radical scavenging ability of DPPH and ABTS, respectively. Deionized water instead of the MAE solution was used as a control, and the free radical scavenging activity was calculated according to Eq. (3):

$$Free\ radical\ scavenging\ activity\ (\%) = \left(1 - \frac{A_1}{A_0}\right) \times 100 \quad (3)$$

where, A_0 is the absorbance value of the control, and A_1 is the absorbance value of samples.

pH sensitivity of MAE

The pH sensitivity was determined by dissolving 2 mg of MAE in 20-mL buffer solutions with varying pH levels (pH 1.0–12.0) for 3 min. Subsequently, each 10-mL solution was transferred into a glass sample vial, and the color change was recorded with a smartphone. Additionally, the visible absorption spectra of the MAE solutions were scanned from 450 to 700 nm using a spectrophotometer (UV mini-124, Shimadzu Corporation, Kyoto, Japan).

Preparation of SG-MAE films

According to our previous study[18], the SG-MAE films were prepared as following: 0.05 mg/mL sodium alginate and gelatin solutions were prepared separately and were mixed at a ratio of 7:3 to prepare SG solution. Then 2, 4, 6, 8, or 10 mg of MAE was added to the mixture, with 1 g glycerol as a plasticizer to obtain film-forming solutions. Then the mixture was treated with an ultrasonic cell grinder (Scientz-IID, SCIENTZ, Ningbo, China) at 500 W for 15 min at 25 °C. After defoaming with a vacuum (Sorvall LYNX 4000, Thermo Fisher Scientific, Waltham, America), each 20-mL film-forming solution was spread onto petri dishes (10 cm × 10 cm) and dried at 25 °C for 24 h to prepare SG-MAE films. These films were marked as SG-2MAE, SG-4MAE, SG-6MAE, SG-8MAE, and SG-10MAE, according to the amount of MAE. The SG film without MAE was used as a control, labeled CK. Before further tests, these films were peeled off and stored at 25 °C and 53% relative humidity for more than 48 h.

Rheological characterization of the film-forming solutions

According to a previous study by Ai et al.[14], the rheological properties of the film-forming solutions were examined using a rheometer (DISCOVERY HR-3, TA Instruments, New Castle, Delaware, USA). The apparent viscosity of the film-forming solution was measured at 25 °C by using a 40-mm aluminum parallel plate with a plate spacing of 1.0 mm, and the shear rate was 0.1–100 s^{-1}. The viscosity (η, Pas) and shear rate (γ, s^{-1}) data were analyzed using a power law model, as shown in Eq. (4):

$$\eta = K\gamma^{n-1} \tag{4}$$

where, K is the consistency index (Pa s^n), and n is the flowing behavior index.

Thickness, water solubility, moisture content, and water vapor permeability

The thickness, water solubility, moisture content, and water vapor transmission rate of the films were determined according to a previous study[14]. The thickness of the films was determined at 10 randomly selected locations in each film using a digital micrometer (digital outside micrometer, GREENER, Yantai, China).

The moisture content (MC) of the film was determined by drying the film at 105 °C until a constant weight W_1 (g) was reaached[16]. The MC was calculated by Eq. (5).

$$MC\ (\%) = \frac{W_0 - W_1}{W_0} \times 100 \tag{5}$$

where, W_0 is the initial weight of the film, and W_1 is the weight of the film after drying.

To detect the water solubility (WS), dried films were weighed (M_0) and put into 50 mL of deionized water under shaking at 25 °C for 24 h. Then the water-insoluble matter was removed and dried at 105 °C to a constant weight (M_1). WS was calculated by Eq. (6).

$$WS\ (\%) = \frac{M_0 - M_1}{M_0} \times 100 \tag{6}$$

The water vapor permeability (WVP) was determined by adding 20 mL of deionized water to a bottle, sealing the bottle with a film sample (4 cm × 4 cm), and placing the bottle in a desiccator for 7 d. We recorded the change in weight of the tubes daily. The procedure was repeated three times for each film. WVP was calculated by Eq. (7).

$$WVP = \frac{\Delta m \times d}{S \times \Delta P \times T} \tag{7}$$

where, Δm is the mass of water transmitted (g), d is the film's thickness (mm), S is the active area of water vapor transmission (3.14×10^{-4} m^2), T is the time (s), and ΔP is the difference in the water vapor between two sides of the film (3.167 kPa) (at 25 °C)[16].

According to Wang et al.[16], the oxygen permeability (OP) was measured by sealing a container containing linoleic acid (2 mL) with the film and then incubating it at room temperature for 7 d. The OP value was calculated using Eq. (8).

$$OP = \frac{\Delta w}{a \times t} \tag{8}$$

where, Δw is the change in the weight of linoleic acid (g), a is the surface area of the film (m^2), and t is the duration (days).

Structural characterization of SG-MAE films

The intermolecular interactions in the films were analyzed using the attenuated total reflection attachment of the infrared spectrometer (Nicolet iS10, Thermo Scientific™, Massachusetts, USA). The measurements were conducted with 32 scans at a resolution of 4 cm^{-1}, covering a wavelength range of 600–4,000 cm^{-1}. Additionally, the crystalline properties of the films were assessed using an X-ray diffractometer (D2 PHASER, Bruker, Karlsruhe, Germany). The X-ray analysis was performed with Cu-Kα radiation at 40 kV at a range of 2θ of 5° to 60° and a scan rate of 4° min^{-1}.

Mechanical properties

A texture analyzer (TA. XTPlus, Stable Micro System, Surrey, UK) equipped with a tensile grips (TG) probe was utilized to determine the mechanical properties, including tensile strength (TS) and elongation at break (EB). The films were cut into long strips with an initial gap of 40 mm and a test speed of 10 mm/s. Each film was tested three times. We calculated TS and EB according to Eqs (9) and (10), respectively.

$$TS\ (MPa) = \frac{F}{w \times d} \tag{9}$$

where, F is the maximum tensile force at break (N), w is the width of the film (mm), and d is the thickness of the film (mm).

$$EB\ (\%) = \frac{L_1 - L_0}{L_0} \tag{10}$$

where, L_1 is the maximum tensile length of the film reached at the time of fracture (mm), and L_0 is the initial length of the clamping distance (mm).

Scanning electron microscopy images of SG-MAE films

The surface and cross-sectional morphologies of the films were characterized using scanning electron microscopy (SEM). The sample was sputter-coated with a layer of gold to enhance conductivity and observed under an accelerating voltage of 3 kV for morphological characterization.

Water contact angle

The water contact angle (WCA) of the films was determined using a video-based optical contact angle-measuring instrument (OCA15EC, Dataphy Instruments Co., Ltd., Dusseldorf, Germany). The films were placed on the sample stage, and 8 μL of deionized water was slowly dispensed onto the film's surface using a 2-mL microsyringe. A digital image of the water droplet was captured using a camera equipped with a macrolens. The WCA (°) was then calculated and recorded using the instrument's software[14].

Transmittance and color properties

The transparency of the films was measured as follows. The films were cut into rectangular strips (4 cm × 1 cm), and their light transmission was scanned at 200–800 nm with a spectrophotometer (UV mini-124, Shimadzu Corporation, Kyoto, Japan).

Their color properties were measured with a portable colorimeter (cs-820N, Hangzhou Caipu Technology Co., Ltd., Hangzhou, China). The following color parameters were measured at five randomly selected locations in each sample: L^* (brightness), a^* (red to green), b^* (yellow to blue), and the total color difference (ΔE) calculated according to Eq. (11)[14]:

$$\Delta E = \sqrt{\left(L^* - L_0^*\right)^2 + \left(a^* - a_0^*\right)^2 + \left(b^* - b_0^*\right)^2} \quad (11)$$

where, L_0^*, a_0^*, and b_0^* are the initial values of the films, and L^*, a^*, and b^* are the values of the films after storage.

Antioxidant activity of SG-MAE films

The antioxidant activity of the films was measured according to a previous study[18]. Briefly, 0.2 g of each film was dissolved in 10 mL ethanol (50% dissolved in water), then the antioxidant activity was measured according to the method of examining the rheological characterization of film-forming solution.

Fish oil packaging

The SG and SG-4MAE films were cut into pouches (4 cm × 4 cm), heat-sealed using a heat-sealing machine (Dapai, Shenzhen Dingsheng Electric Appliance Co., LTD., Shenzhen, China), and sealed to pack 2 g of fish oil. The effect of top-cover packaging on the fish oil was also investigated: 10 mL of edible oil in a glass bottle was covered with a SG or SG-4MAE film (4 cm × 4 cm) and then fixed with a rubber band. Unpackaged fish oil and fish oil in ziplock bags were used as controls. All the samples were stored at 25 ± 3 °C and 53% ± 2% relative humidity for 4 weeks. To quantitatively assess the extent of oxidation, the peroxide value (POV), thiobarbituric acid value (TBA), and acid value (AV) of the fish oil were measured weekly.

Evaluation of fish oil's quality during storage

Peroxide value

According to Zhu et al.[19], 1 g of fish oil, 30 mL of trichloromethane/acetic acid (3:2 volume ratio), and 1 mL of saturated potassium iodide were mixed in a conical flask. The mixture was homogenized and reacted in the dark for 3 min. Then 100 mL of distilled water was added, and the reaction mixture was titrated with a 0.01 mol/L sodium thiosulfate solution, using a 1 mL soluble starch solution (1%, w/w) as an indicator. A blank titration was conducted in the same way without the oil sample. POV (mmol/kg) was calculated using Eq. (12).

$$POV = \frac{(V - V_0) \times c}{2m} \times 1{,}000 \quad (12)$$

where, V and V_0 are the volume of sodium thiosulfate solution (mL) consumed by the sample and the blank solution, respectively; c is the concentration of the sodium thiosulfate standard solution (mol/L); and m is the weight of fish oil (g).

Thiobarbituric acid value

Samples of 50–250 mg of fish oil were mixed with 25 mL of 1-butanol, then the 5-mL mixture was reacted with 5 mL of TBA reagent at 95 °C for 2 h. After heating, these tubes were rapidly cooled in an ice-water bath to terminate the reaction and prevent further oxidation[19]. The absorbance of the samples at 530 nm was tested, and the TBA value was calculated via Eq. (13).

$$TBA = \frac{50 \times (A - B)}{m} \quad (13)$$

where, A is the sample absorbance, B is the blank absorbance, and m is the weight of fish oil (mg).

Acid value

According to the method of Wang et al.[20], 0.5 g of fish oil was mixed with 50 mL of ether/isopropanol (1:1, volume ratio). The mix was then titrated using 0.001 mol/L NaOH solution with phenolphthalein as an indicator. A blank titration was treated in the same way without oil. AV (mg/g) was calculated by using Eq. (14).

$$AV = \frac{(V - V_0) \times c \times 40}{m} \quad (14)$$

where, V and V_0 are the volume of the NaOH solution (mL) consumed by the sample and blank solution, respectively; c is the concentration of the NaOH standard solution (mol/L); 40 is the molar mass of NaOH (g/mol); and m is the weight of fish oil (g).

Shelf life prediction

The patterns of change in the quality of food usually conform to zero- or one-level models, so the oxidation kinetic equations for fish oil during storage at 25 °C were established using Eq. (15)[21]. The end of shelf life was predicted and calculated as the acid value of fish oil reaching 3 mg/g.

$$\ln(AV) = kt + a \quad (15)$$

where, AV is the acid value of edible oil at t days of storage (mg/g), k is the rate constant of oxidative rancidity (1/d), t is the number of days of storage (days), a is ln (AV_0), and AV_0 is the initial acid value.

Statistical analysis

The results are reported as the mean ± standard deviation. Data were subjected to one-way analysis of variance (ANOVA) by SPSS 24 software (IBM, New York, USA) according to Duncan's multiple range tests ($p < 0.05$). A significance level of $p < 0.05$ was used to determine statistical significance.

Results and discussion

Characterization of MAE

Prior to incorporating anthocyanins into SG films, anthocyanins from mulberry pomace were extracted and purified. The contents of total phenols and anthocyanins in the crude extract were 7.27 ± 0.42 and 3.36 ± 0.43 mg/g, respectively. After being purified with the AB-8 macroporous resin column, there were 296.86 ± 6.92 mg/g total

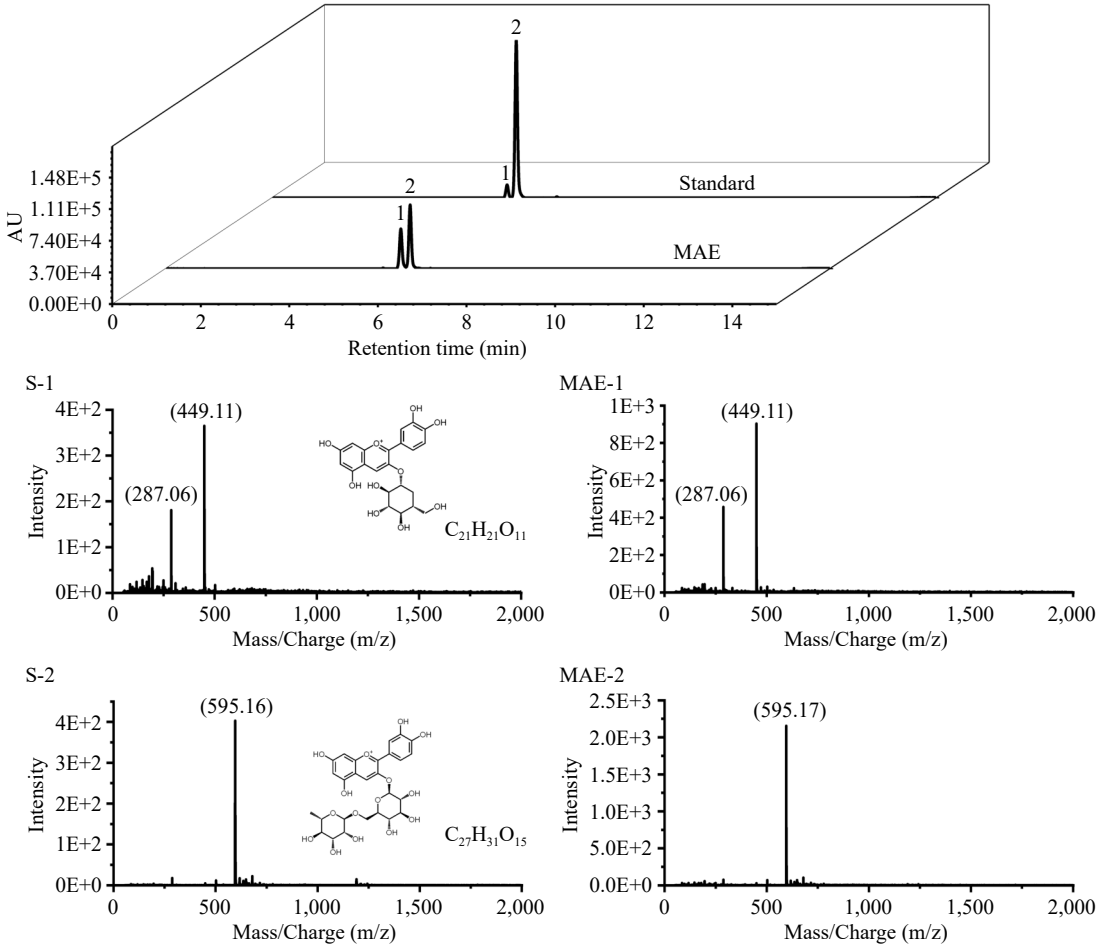

Fig. 1 The UPLC chromatograms (520 nm) and mass spectrometry of Peak 1 (S-1, MAE-1) and Peak 2 (S-2, MAE-2) of anthocyanins in MAE and the anthocyanin standard.

polyphenols and 146.50 ± 2.35 mg/g anthocyanins in MAE. According to the result from UPLC-MS analysis, cyanidin-3-glucoside (Peak 1, retention time = 5.32 min, M = 449) and cyanidin-3-rutinoside (Peak 2, retention time = 5.52 min, M = 595) were the two major anthocyanins in MAE (Fig. 1). Similarly, the four major anthocyanins in mulberries include cyanidin-3-glucoside, cyanidin-3-rutinoside, cyanidin-3,5-diglucoside, and pelargonidin-3-glucoside[22].

As they were exposed to a wide pH range (pH 1.0–12.0), the MAE solutions showed obvious changes in color (Fig. 2a). The solution was red at pH 1–3, pink at pH 4–6, light purple at pH 7–8, dark brown at pH 9–10, and yellow at pH 12. The phenomenon can be explained by the anthocyanins in MAE undergoing structural alteration with increasing pH. Generally, anthocyanins change from flavylium cations (red) to quinoidal anhydrobase (purple), and finally to a chalcone structure (yellow-green)[15]. Figure 2a shows the UV–visible absorption spectra of MAE in different pH buffers (1.0–12.0). In the visible range (400–750 nm), the maximum absorption peak of MAE at pH 1–3 was at 510 nm. With a further increase in pH, the absorption peak shifted to larger wavelengths, a phenomenon known as redshift[23]. A similar phenomenon was observed in anthocyanin from grape skins, as its UV–visible absorption peak shifted from 518 to 618 nm with a change in pH across 4–10[24].

The antioxidant activity of MAE is positively related to the dose (Fig. 2b). The excellent antioxidant activity of MAE is attributed to its aromatic rings and the hydroxyl groups of cyanidin-3-glucoside and cyanidin-3-rutinoside. The hydroxyl groups form more stable semiquinone radicals, which may help inhibit free radical chain reactions. These results further substantiated the potential applicability of adopting MAE in biodegradable films as active packaging materials.

Physicochemical characterization of SG-MAE films

Rheology of the film-forming solutions

Rheology refers to the deformation and flow characteristics of film-forming solutions under the action of external forces[14]. As shown in Fig. 3a, the shear rate and viscosity of the film-forming solutions showed a close linear relationship, exhibiting pseudoplastic behavior. This phenomenon may be caused by the disruption of the film-forming solutions' network structure with increasing shear rate, thereby reducing viscosity. The initial viscosity of SG-MAE films elevated with the addition of MAE, which increased with the amount of MAE added. This could be attributed to the potential formation of more hydrogen bonds or other noncovalent interactions between MAE and SG, which enhanced the network structure of the films, leading to higher viscosity. However, the viscosity began to decrease when more than 0.8 mg/mL MAE added. This may be related to the disruption of hydrogen bonds between sodium alginate and gelatin. Nevertheless, the decrease indicates that elevated viscosity hinders the uniform dispersion of the components and the removal of visible air bubbles during film preparation,

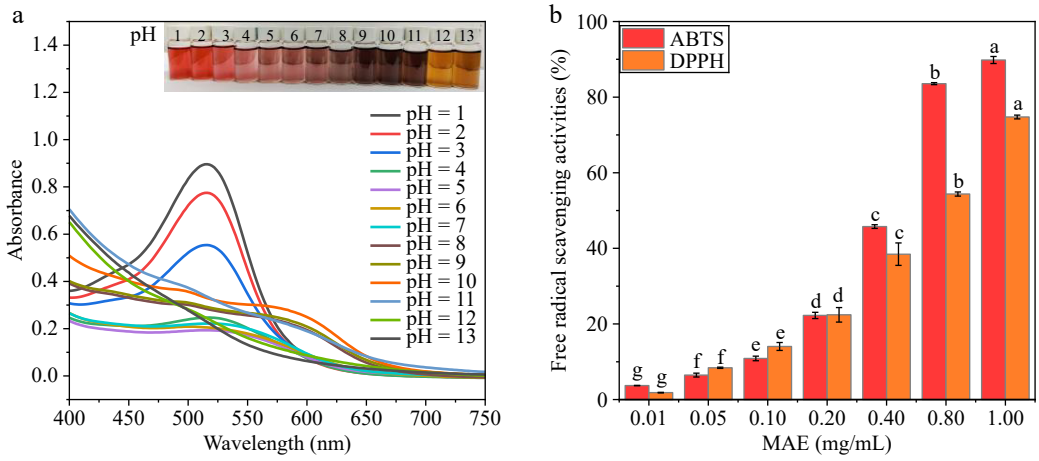

Fig. 2 (a) The UV–visible spectroscopy of mulberry pomace anthocyanin extract (MAE) and (b) its free radical scavenging activity against ABTS and DPPH. Different letters on the columns indicate statistically significant differences among MAE concentrations ($p < 0.05$).

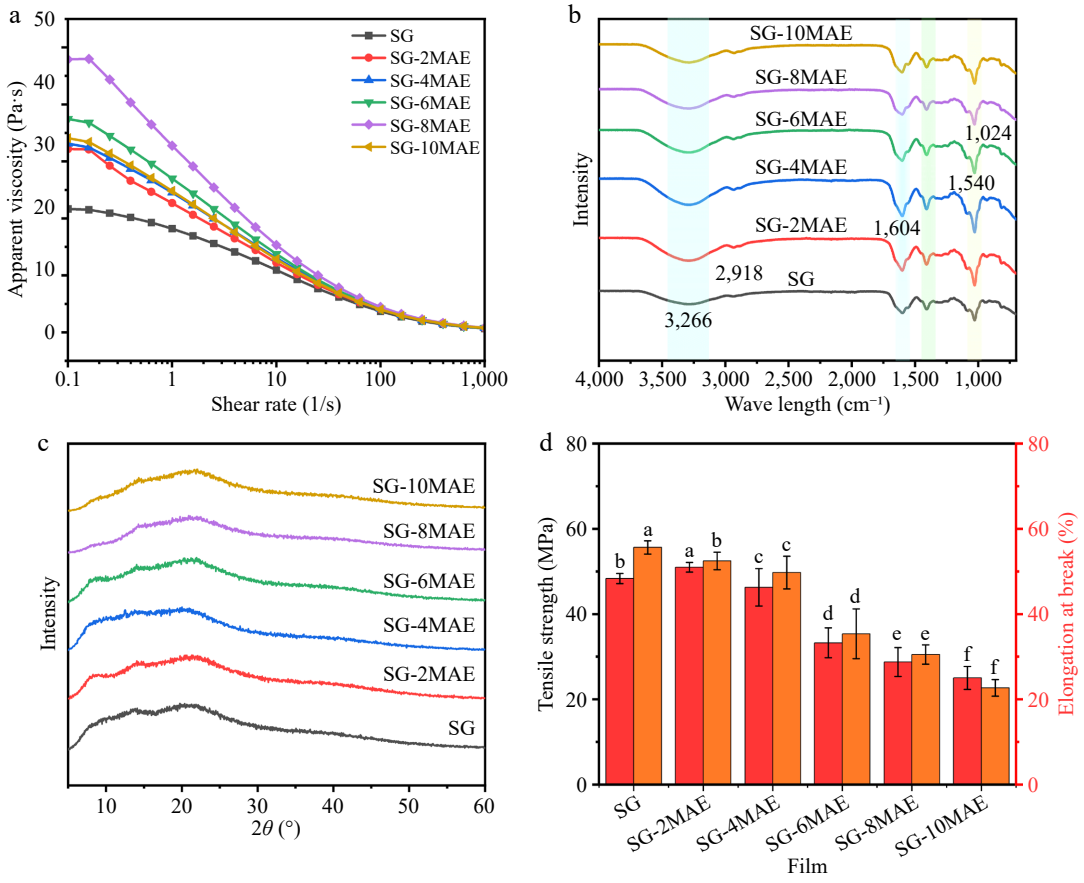

Fig. 3 The (a) rheological properties, (b) Fourier transform infrared, (c) X-ray diffraction, and (d) mechanical properties of SG-MAE films. SG: sodium alginate–gelatin film; SG-(2-10) MAE, sodium alginate–gelatin film with 0.2–1.0 mg/mL MAE.

thereby leading to a lack of continuous smoothness in the film[25]. Thereby, 0.2–0.6 mg/mL MAE would be recommended for preparing films.

Thickness, moisture content, water solubility, and water vapor permeability

As shown in Table 1, no significant effect of 0.2–0.8 mg/mL MAE on the film's thickness was observed ($p > 0.05$). The moisture content of SG-MAE films was lower than that of SG film ($p < 0.05$), which may be caused by the interaction between MAE and SG molecules, reducing the number of available hydroxyl groups and thus the possibility of combining with water. Moreover, the mixing of film-firming matrices leads to a sharp decrease in water solubility, which might result in a complex, hydrophobic, and dense network. A similar phenomenon was observed by Gasti et al.[26], where a chitosan–methylcellulose–*Phyllanthus reticulatus* film was prepared. Films used for food packaging should have good water vapor and oxygen barrier properties to reduce microbial growth and oxidative deterioration[27]. As shown in Table 1, the WVP of SG films was 2.21 ± 0.01 × 10^{-11} g/(m·s·Pa), and that of SG-MAE films was lower ($p <$

Table 1. Physical properties of SG-MAE films.

Films	Thickness (μm)	Water solubility (%)	Moisture content (%)	Water vapor permeability ($\times 10^{-11}$ g/[m·s·Pa])	Oxygen permeability (g/dm^2)
SG	80.12 ± 4.11^{c}	63.11 ± 0.77^{a}	19.58 ± 1.62^{a}	2.21 ± 0.01^{a}	3.16 ± 0.21^{c}
SG-2MAE	82.69 ± 3.29^{c}	62.89 ± 2.31^{a}	17.83 ± 1.68^{b}	1.50 ± 0.01^{d}	5.22 ± 0.54^{b}
SG-4MAE	80.07 ± 2.71^{c}	62.31 ± 1.23^{a}	16.11 ± 1.57^{c}	1.73 ± 0.03^{c}	5.43 ± 0.67^{b}
SG-6MAE	85.61 ± 4.21^{b}	60.03 ± 0.91^{b}	16.53 ± 2.36^{c}	1.85 ± 0.01^{b}	5.51 ± 0.61^{b}
SG-8MAE	83.09 ± 2.81^{bc}	58.21 ± 0.89^{c}	18.73 ± 0.82^{ab}	1.97 ± 0.17^{ab}	5.47 ± 0.35^{b}
SG-10MAE	89.93 ± 1.01^{a}	58.11 ± 0.77^{c}	17.42 ± 0.80^{b}	1.65 ± 0.01^{bc}	6.20 ± 0.23^{a}

SG-MAE, sodium alginate–gelatin film with 0.2–1.0 mg/mL mulberry pomace anthocyanin extract. Different letters in the same column represent significant differences at $p < 0.05$.

0.05). The OP of SG films was 3.16 ± 0.21 g/dm^2, which was significantly lower than in the SG-MAE films ($p < 0.05$). This may be a result of the nonpolar components of MAE, which increase the solubility of oxygen[28]; furthermore, the polar molecules of MAE are embedded among the polymer chains of sodium alginate–gelatin. Through interactions such as hydrogen bonding, these molecules 'expand' the polymer network, increasing the free volume and thus providing more pathways for oxygen diffusion, which leads to an increase in oxygen permeability. Thereby, 0.2–0.6 mg/mL MAE would be recommended, considering the acceptable WVP and OP of SG-MAE films.

Fourier transform infrared and X-ray diffraction spectroscopy

The infrared spectra of SG-MAE films with 0.2–1.0 mg/mL MAE shows characteristic bands at 3,286, 2,927, 1,604, 1,552–1,540, and 1,029 cm^{-1}, attributed to the O-H stretching vibration, C-H stretching, C=C stretching vibration, N-H group bending vibration, C-N group stretching vibration, and C-H bending vibration, respectively. Similarly, the SG films exhibited distinct peaks at 3,266, 2,918, 1,604, 1,540, and 1,407 cm^{-1}, corresponding to O-H stretching vibration, C-H and C-H$_2$ stretching and bending vibration, esterification carboxyl stretching vibration, and asymmetric stretching vibration, respectively[29]. The changes in the vibrational stretching peak intensified upon the addition of MAE into SG matrices. Additionally, the peak at 3,266 cm^{-1} (the amide-A band) shifted to 3,286 cm^{-1}, suggesting hydrogen bonding interactions between the MAE and SG matrices, consistent with Ding et al.[30]. The absorption peaks at 1,604 cm^{-1} and the shift from 1,029 to 1,018 cm^{-1} correspond to the C-C stretching vibration of aromatic compounds and the deformation vibration of phenolic hydroxyl (C-OH), respectively, which is consistent with the addition of MAE[31]. Overall, the results show the excellent incorporation of MAE into the SG film.

X-ray diffraction (XRD) patterns are commonly used to analyze the crystal structure, molecular arrangement, and crystallinity of films. As shown in Fig. 3c, all film samples showed a distinct broad peak at 2θ of about 20°. MAE's incorporation introduced no new XRD peaks, indicating uniform anthocyanin dispersion and full compatibility between SG and MAE. A similar result was observed in the anthocyanin-loaded PLA/quaternized chitosan films by Xu et al.[32]. These results suggest that the addition of MAE avoided structural changes and maintained the crystalline phase within the new composite film.

Mechanical properties

The TS of packaging film must be more than 30 MPa, and EB should be at least 20%. As shown in Fig. 3d, the TS and EB properties of SG films were significantly affected by the MAE dose ($p < 0.05$). The TS and EB of the SG films were 48.33 MPa and 55.62%, respectively. With the addition of 0.2 mg/mL MAE (SG-2MAE), the TS of the films increased to 50.98 MPa ($p < 0.05$), attributed to the fact that anthocyanins may act as plasticizers or cross-linkers in the SG film-forming solution. In this case, the interaction force with the polymer molecule chains increased, resulting in the more compact structure of the films with a higher TS[33]. A further increase in the MAE dose (0.4–1.0 mg/mL) led to significant decreases in the TS and EB of these films ($p < 0.05$). This is because the anthocyanins may cross-link with each other through forces such as hydrogen bonding or excessive cross-linking with the polymer chains of SG. This may lead to the film becoming too rigid, thus reducing its ductility and toughness, and may even make the film brittle, affecting its mechanical properties. A similar phenomenon was reported by Wu et al.[34], when red kale anthocyanins were added to oxidized chitin nanocrystals–konjac glucomannan matrices. Therefore, a moderate amount of anthocyanins might enhance the mechanical properties of films. However, too high a dose of anthocyanins may lead to excessive cross-linking, thus reducing the ductility and toughness of the films and ultimately worsening their mechanical properties.

SEM of SG-MAE films

The surface and cross-sectional morphologies of the films were examined using SEM. As shown in Fig. 4a, the SG film without MAE exhibited a relatively uniform surface with minimal pores or cracks, though some aggregates were observed, likely because of incomplete miscibility between sodium alginate and gelatin. However, increased light-colored protrusions and raised spots appeared on the SG-MAE films. MAE interacts with sodium alginate and gelatin via hydrogen bonding and hydrophobic interactions, promoting the migration of hydrophobic components toward the surface during drying. Similar irregular aggregates have been reported elsewhere[35]. Cross-sectional images revealed that the SG film was largely pore-free, whereas the SG-MAE films showed increased surface roughness, cracks, delamination, and porosity, indicating reduced structural homogeneity. These changes were consistent with the observed decrease in TS when more than 0.2 mg/mL MAE was added. The results suggest that adding excessive amounts of MAE promotes phase separation, leading to crack propagation and porous morphology in the films.

Water contact angle

The WCA is a key parameter for evaluating films' wettability, reflecting the strength of the interaction between water and the film's surface. As shown in Fig. 4b, the WCA of the SG films is 109°, showing their hydrophobic characteristic. With the incorporation of MAE, the WCA of SG-MAE films decreased ($p < 0.05$), and the decrease was dose-related. The WCA of SG-6MAE films was lower than 90°, indicating hydrophilicity. The transition from hydrophobicity to hydrophilicity resulted from the abundant hydroxyl groups in anthocyanins supplying extremely high water absorption[36]. The hydrophilic groups of MAE were enriched or reoriented on the surface of the membrane. A similar phenomenon in an anthocyanin–polyvinyl acetate–sodium alginate film was reported by Qi

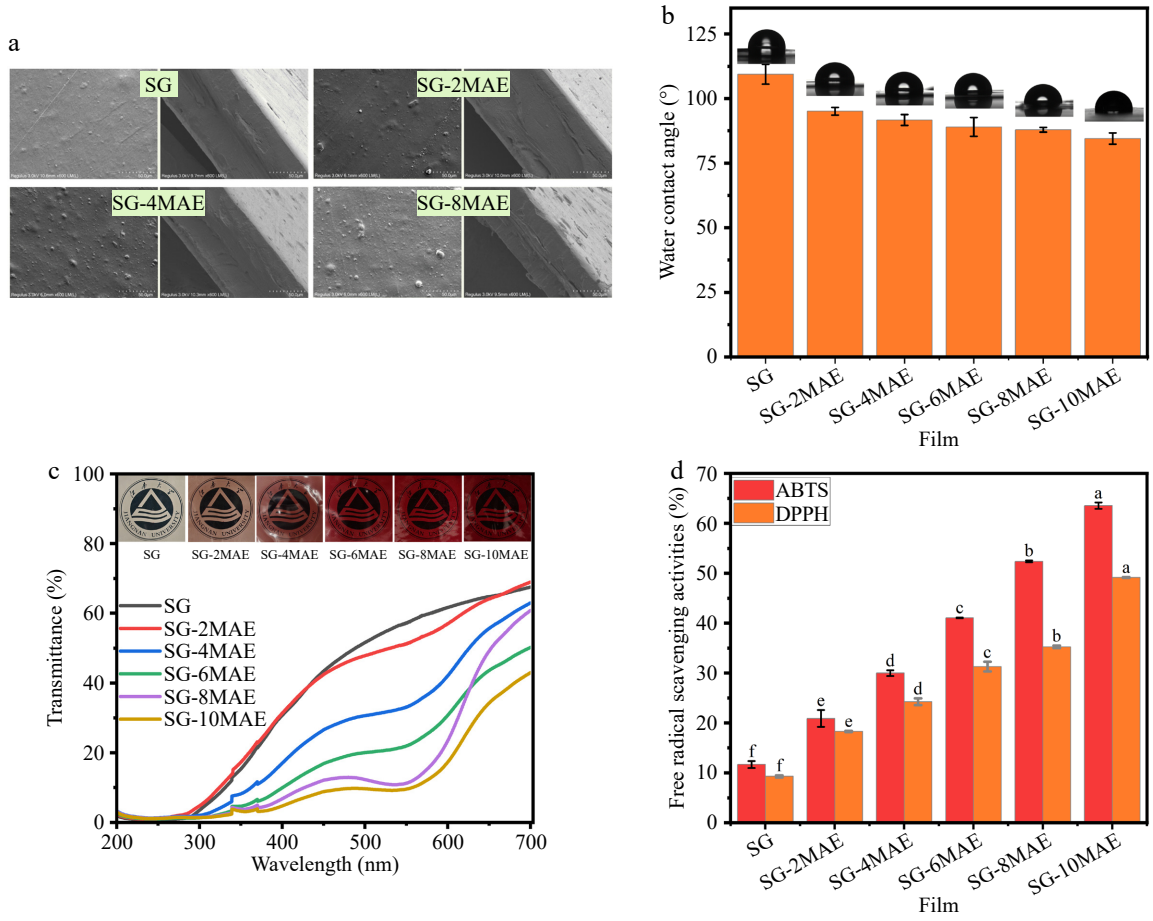

Fig. 4 The (a) SEM, (b) WCA, (c) transmittance scanning spectra, and (d) free radical scavenging activities of SG-MAE films. SG, sodium alginate–gelatin film; SG-(2-10) MAE, sodium alginate–gelatin film with 0.2–1.0 mg/mL MAE.

Table 2. Optical properties of SG-MAE films.

Films	*L**	*a**	*b**	Δ*E*	$T_{(600\ nm)}$ (%)
SG	90.94 ± 0.26^{a}	−0.75 ± 0.30^{f}	15.14 ± 0.20^{a}	–	71.84 ± 0.98^{a}
SG-2MAE	76.14 ± 1.50^{b}	10.26 ± 0.33^{e}	13.87 ± 0.29^{b}	26.46 ± 1.46^{e}	58.77 ± 0.55^{b}
SG-4MAE	64.78 ± 0.61^{c}	20.23 ± 0.00^{d}	14.59 ± 0.38^{a}	40.2 ± 1.33^{d}	47.63 ± 1.85^{c}
SG-6MAE	56.28 ± 1.27^{d}	24.46 ± 0.78^{c}	15.06 ± 0.29^{a}	49.89 ± 1.79^{c}	40.34 ± 0.97^{d}
SG-8MAE	43.32 ± 3.03^{e}	30.19 ± 0.53^{b}	15.26 ± 0.58^{a}	63.35 ± 2.56^{b}	28.55 ± 1.60^{e}
SG-10MAE	36.92 ± 0.05^{f}	36.29 ± 0.80^{a}	16.13 ± 0.77^{a}	71.93 ± 0.57^{a}	22.3 ± 0.14^{f}

SG-MAE, sodium alginate–gelatin film with 0.2–1.0 mg/mL MAE. Different letters in the same column represent significant differences at $p < 0.05$.

et al.[35], where the WCA of the film decreased significantly from 56.69° to 48.38° with anthocyanin, increasing the hydrophilicity.

Color and transmittance properties

Color and opacity affect consumer acceptance and the barrier properties of the film. As shown in Table 2, the *L**, *a**, and *b** values of the SG films were 90.94 ± 0.26, −0.75 ± 0.3, and 15.14 ± 0.2, respectively. With MAE, the *a** and *L** values of SG-MAE films changed significantly ($p < 0.05$), showing a red color. The color properties of SG-MAE films varied with the MAE dose. Since both SG and gelatin are yellowish, and glycerol is colorless and transparent, the change is mainly attributed to the color response of MAE. Cao et al.[37] found out that with more black nightshade anthocyanins in films, *L** significantly decreased, whereas *a**, *b**, and Δ*E* increased, with the films tending to be reddish.

As shown in Fig. 4c, the transmittance of SG films at 600 nm reduced significantly with MAE ($p < 0.05$). This reduction indicated the enhanced UV-blocking properties of SG-MAE films resulting from the introduction of MAE. Gao et al.[25] found that films of acetylated tapioca starch–carboxymethylcellulose containing black rice anthocyanin extracts had good UV-blocking properties, which were mainly caused by the presence of several chromophores in the structure of anthocyanins (e.g., C=O bonds and C=C bonds) as well as phenolic compounds that absorb UV radiation. Films with high UV-blocking properties can be used for packaging edible oils to reduce photo-oxidative decomposition. However, the gradual color deepening of the film may affect the aesthetics of the product and consumer acceptance.

Antioxidant capacity of SG-MAE films

Generally, oxidation of unsaturated fatty acids in edible oils is undesirable, so the antioxidant activity of SG-MAE films was evaluated (Fig. 4d). The SG film showed the weakest antioxidant activities: Its

antioxidant activities against ABTS and DPPH radicals were 11.67% and 9.29%, which were mainly provided by amino acids or small-molecule peptides in gelatin. The addition of MAE significantly increased the antioxidant activity ($p < 0.05$). This were previously confirmed by the antioxidant activities of MAE itself. Furthermore, the phenolic hydroxyl group (-OH) of the two major anthocyanins identified in MAE (cyanidin-3-glucoside and cyanidin-3-rutinoside) reduces $ABTS^+$ to stable ABTS by providing hydrogen atoms (H), and anthocyanins themselves are oxidized to anthocyanin oxides[38]. Similar to the $ABTS^+$ reaction, the phenolic hydroxyl group in anthocyanins scavenge DPPH radicals by transferring hydrogen atoms or electrons[39]. The reason for the different antioxidant activities of MAE films against ABTS and DPPH free radicals may be caused by the higher stability of DPPH, which reacts with polyphenols (catechins, proanthocyanidins) but not phenolic acids or sugars, whereas ABTS is highly reactive and therefore able to react with a wider range of antioxidants[40]. A previous study found that anthocyanins from different sources increase the antioxidant activity of packaging films[32]. These results indicated that SG-MAE films might have potential in protecting packaged fish oil from oxidative degradation, thus extending its shelf life and maintaining its edibility.

According to these observations, since more MAE leads to decrease in the mechanical strength of SG-MAE films, which is unfavorable for food packaging, a balance should be achieved in MAE content when considering the appearance, mechanical properties, hydrophobic characteristics, and antioxidant performance of the films, rather than solely pursuing a high anthocyanin concentration. After comprehensive consideration, SG-4MAE was identified as the optimal choice for subsequent application in edible oil packaging tests.

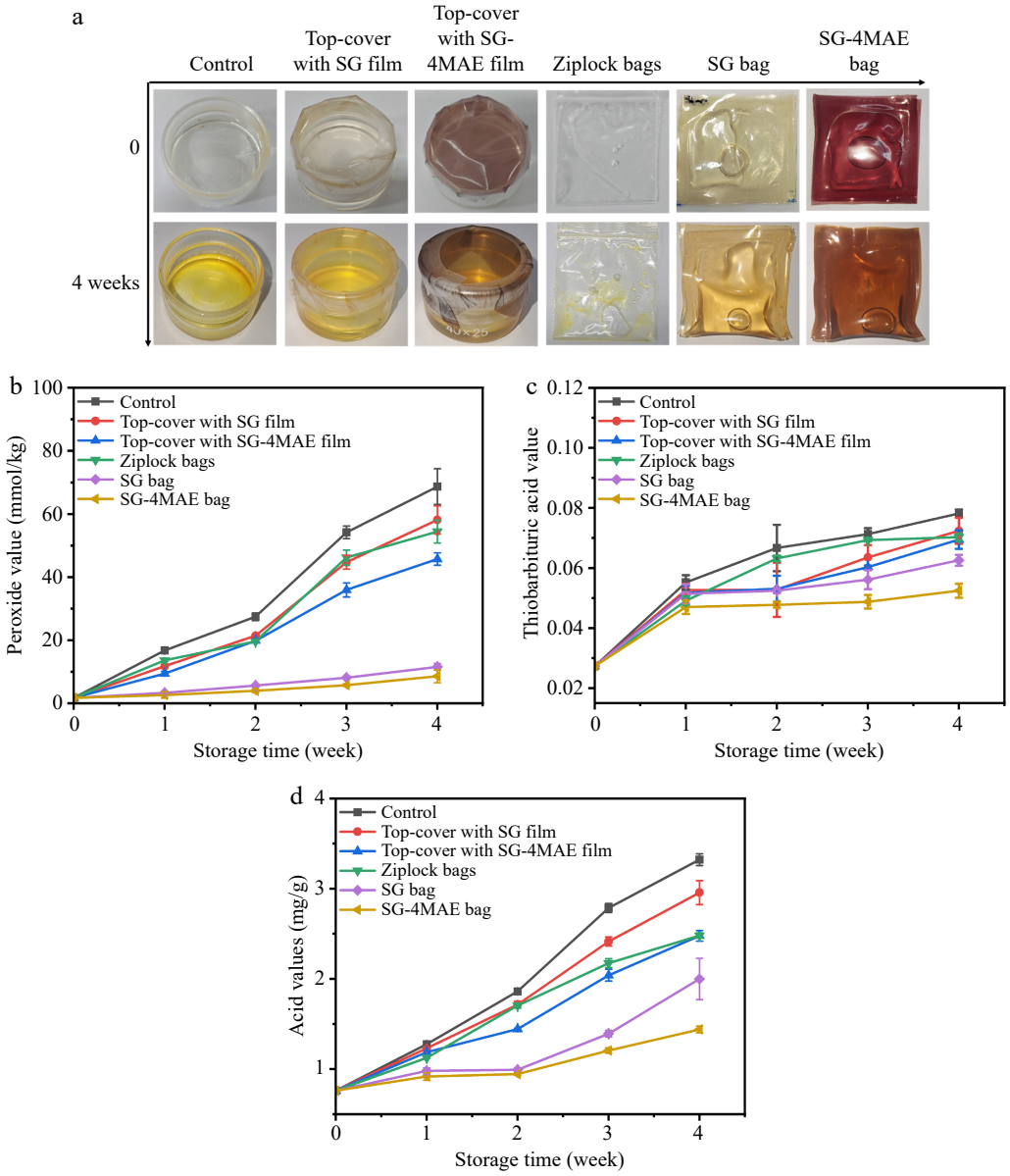

Fig. 5 (a) The packaging of fish oil, (b) peroxide values, (c) TBA values, and (d) acid values of fish oil with different packaging methods during storage at 25 °C. Control: Sample of unpackaged fish oil; ziplock bags: Fish oil packaged using ziplock bags; SG: Fish oil packaged using sodium alginate–gelatin (SG) film in the forms of bags and top-covering; SG-4MAE: Fish oil packaged in the forms of bags and top-covering using sodium alginate–gelatin film containing 0.4 mg/mL MAE.

Application of SG-4MAE films for fish oil packaging and preservation

As shown in Fig. 5a, a progressive yellow darkening was visually observed in all fish oil samples during storage, which is attributed to the accumulation of colored oxidation products, such as conjugated dienes and ketones, derived from polyunsaturated fatty acid oxidation. POV is one of the most commonly used indexes to evaluate the oxidation rancidity of oils and fats. As shown in Fig. 5b, the POV of unpackaged fish oils increased significantly during storage (from 1.73 to 68.68 mmol/kg). This phenomenon can be attributed to the high unsaturated fatty acid content in fish oil, which is prone to oxidize, especially when directly exposed to air, where oxygen can penetrate the oil molecules more efficiently and promote oxidation reactions[41]. Compared with the control group, the oxidation of fish oil packaged in ziplock bags or top-covered with SG or SG-4MAE films was delayed (Fig. 5b). However, the oxidation reaction still occurred. Notably, the POV of fish oil packaged with SG or SG-4MAE bags was obviously lower and with a much slow rising trend over 4 weeks. The trend indicated that the SG-4MAE bag in particular inhibited the auto-oxidation of fish oil. Compared with ziplock bag packaging, the active film packaging isolates oxygen more effectively and may further reduce the occurrence of oxidation reactions through the release of antioxidant substances or adsorption of oxygen, thus significantly reducing the degree of oxidative rancidity[20]. This result is consistent with our previous findings regarding sunflower oil and lard packaging, and further demonstrates the effectiveness of active film packaging in preserving edible oils[18].

The TBA is another important indicator for assessing the oxidation of fish oil, which mainly reflects the content of aldehydes (e.g., malondialdehyde), which are the oxidation products of unsaturated fatty acids. As shown in Fig. 5c, the TBA of all the samples increased, indicating the inevitable oxidization of fish oil during storage. However, after 4 weeks, the TBA of fish oil packaged in the SG-4MAE bag changed the least (0.052 mg/g), indicating that this packaging can effectively isolate oxygen, inhibit the generation of oxidation products with the antioxidant effect of anthocyanins, and reduce the generation of harmful substances such as malondialdehyde.

The main causes of rancidity in edible oils are usually hydrolysis and oxidation reactions. The hydrolysis reaction is the process by which the triglyceride molecules in edible oils interact with water to produce free fatty acids and glycerol[20]. However, the hydrolysis reaction has a very limited effect, since edible oils themselves have a very low moisture content, and do not contact external moisture in a sealed packaging environment. Therefore, the increase in the AV of fish oil was mostly related to an oxidation reaction, which was triggered by the reaction between the oil and oxygen in the air, especially in the oils with a high content of unsaturated fatty acids. As shown in Fig. 5d, the AV of the fish oil without packaging (the control), the fish oil packaged in a ziplock bag, and the fish oil in a SG film bag was 130.7%, 72.3% and 38.9% higher than that packaged in a SG-4MAE bag after 4 weeks, respectively. This indicates that SG-4MAE film effectively prevented the oxidative rancidity of fish oil. Luo et al.[42] found that by adding blueberry anthocyanins to camellia seed oil, the oxidation stability at high temperatures improved, and the content of free fatty acids reduced. Therefore, incorporating anthocyanins into degradable films has great antioxidant potential for packaging fish oil.

Through the kinetic equation, the shelf life of fish oil with different types of packaging can be calculated. As shown in Table 3, the oxidation reaction of fish oil during storage conforms to the first-order kinetic reaction. The shelf life of fish oil was extended by 6 d when packaged in ziplock bags compared with the control, which was extended to 43 d with the SG bag. This type of packaging can delay the oxidation of fish oil by reducing the entry of oxygen and controlling the entry of moisture into the packaging. Encouragingly, the shelf life of fish oil was 63 d with the SG-4MAE bag. This result indicates that direct packaging with SG-4MAE film has good performance in terms of oxygen insulation, moisture resistance, and oxidation resistance, which can effectively inhibit the oxidation reaction of fish oil and extend its shelf life. Therefore, the SG-4MAE bag showed the best potential for packaging fish oil. Further studies to improve the palatability of the SG-4MAE film should be conducted.

Table 3. Kinetic analysis and predicted shelf life of fish oil packaged with SG-4MAE films.

Packaging	Kinetic equation	R^2	Shelf life (days)
Control	$\ln(AV) = 0.053t - 0.173$	0.97	24.6
Top-cover with SG film	$\ln(AV) = 0.048t - 0.170$	0.97	26.5
Top-cover with SG-4MAE film	$\ln(AV) = 0.042t - 0.223$	0.99	31.6
Ziplock bags	$\ln(AV) = 0.043t - 0.196$	0.96	30.3
SG bag	$\ln(AV) = 0.033t - 0.315$	0.95	42.8
SG-4MAE bag	$\ln(AV) = 0.022t - 0.282$	0.95	62.6

Control: Unpackaged fish oil; ziplock bags: Fish oil packaged in plastic ziplock bags; SG bag and SG-4MAE bag: Fish oil packaged in bags made of sodium alginate–gelatin (SG) film and sodium alginate–gelatin film containing 0.4 mg/mL mulberry pomace anthocyanin extract; top-covering with SG film and SG-4MAE film: Fish oil packaged in glass bottles and covered with SG or SG-4MAE films.

Conclusions

In this study, a novel antioxidant packaging film was developed using SG as a film-forming substrate, with MAE serving as an active component to inhibit the oxidation of fish oil. Cyanidin-3-glucoside and cyanidin-3-rutinoside in MAE endowed the film with a reddish color and improved the UV-blocking properties. Moreover, MAE contains rich phenolic hydroxyl structures, which enhance the antioxidant property of the film, which exhibited strong scavenging activity against ABTS and DPPH. Furthermore, the favorable mechanical properties, hydrophobic characteristics, and antioxidant performance of SG-4MAE film resulted in significantly delayed oxidation of fish oil after 4 weeks' storage. Thus, this SG-4MAE film provides a novel strategy for packaging fish oil.

Author contributions

The authors confirm their contributions to the paper as follows: writing – review & editing: Lv Y; draft manuscript preparation: Lv Y, Yang J, Luo T; investigation: Lv Y, Liao H; methodology: Yang J, Liao H; conceptualization, supervision, project administration, funding acquisition: Liao H. All authors reviewed the results and approved the final version of the manuscript.

Data availability

The datasets generated during and/or analyzed in the current study are available from the corresponding author on reasonable request.

Acknowledgments

This work was supported by the Innovation and Entrepreneurship Training Program for College Students in Jiangsu Province (Grant No. 202410295126Y).

Conflict of interest

The authors declare that they have no known competing financial interests or personal relationships that could have appeared to influence the work reported in this paper.

Dates

Received 8 December 2025; Revised 3 March 2026; Accepted 3 March 2026; Published online 30 March 2026

References

[1] Ruan P, Zhang K, Zhang W, Kong Y, Zhou Y, et al. 2024. Polyphenolic truxillic acid crosslinked sodium alginate film with notable antimicrobial and biodegradable properties for food packaging. *International Journal of Biological Macromolecules* 279:135184

[2] Stevenson M, Long J, Seyfoddin A, Guerrero P, de la Caba K, et al. 2020. Characterization of ribose-induced crosslinking extension in gelatin films. *Food Hydrocolloids* 99:105324

[3] Abdelhedi O, Salem A, Nasri R, Nasri M, Jridi M. 2022. Food applications of bioactive marine gelatin films. *Current Opinion in Food Science* 43:206–215

[4] Noh SW, Song DH, Yang NE, Kim HW. 2023. Incorporation of soy protein isolate and egg-white protein to improve nutritional value and hardness of gelatin gels for the elderly. *Food Bioscience* 53:102806

[5] Luo Q, Hossen MA, Zeng Y, Dai J, Li S, et al. 2022. Gelatin-based composite films and their application in food packaging: a review. *Journal of Food Engineering* 313:110762

[6] López-Pedrouso M, Lorenzo JM, Franco D. 2022. Advances in natural antioxidants for food improvement. *Antioxidants* 11:1825

[7] Abdel-Aal EM, Hucl P, Rabalski I. 2018. Compositional and antioxidant properties of anthocyanin-rich products prepared from purple wheat. *Food Chemistry* 254:13–19

[8] Wang S, Xia P, Wang S, Liang J, Sun Y, et al. 2019. Packaging films formulated with gelatin and anthocyanins nanocomplexes: physical properties, antioxidant activity and its application for olive oil protection. *Food Hydrocolloids* 96:617–624

[9] Zhang MQ, Zhang J, Zhang YT, Sun JY, Prieto MA, et al. 2023. The link between the phenolic composition and the antioxidant activity in different small berries: a metabolomic approach. *LWT* 182:114853

[10] Yum HW, Kim SH, Kang JX, Surh YJ. 2018. Amelioration of UVB-induced oxidative stress and inflammation in fat-1 transgenic mouse skin. *Biochemical and Biophysical Research Communications* 502:1–8

[11] Killeen DP, Marshall SN, Burgess EJ, Gordon KC, Perry NB. 2017. Raman spectroscopy of fish oil capsules: polyunsaturated fatty acid quantitation plus detection of ethyl esters and oxidation. *Journal of Agricultural and Food Chemistry* 65:3551–3558

[12] Kurek M, Ščetar M, Nuskol M, Janči T, Tanksoić M, et al. 2024. Assessment of chitosan/gelatin blend enriched with natural antioxidants for antioxidant packaging of fish oil. *Antioxidants* 13:707

[13] Miyashita K, Uemura M, Hosokawa M. 2018. Effective prevention of oxidative deterioration of fish oil: focus on flavor deterioration. *Annual Review of Food Science and Technology* 9:209–226

[14] Ai Y, Wang G, Fang F, Zhang F, Liao H. 2022. Development of real-time intelligent films from red pitaya peel and its application in monitoring the freshness of pork. *Journal of the Science of Food and Agriculture* 102:5512–5522

[15] Etxabide A, Yang Y, Maté JI, de la Caba K, Kilmartin PA. 2022. Developing active and intelligent films through the incorporation of grape skin and seed tannin extracts into gelatin. *Food Packaging and Shelf Life* 33:100896

[16] Wang F, Xie C, Tang H, Hao W, Wu J, et al. 2023. Development, characterization and application of intelligent/active packaging of chitosan/chitin nanofibers films containing eggplant anthocyanins. *Food Hydrocolloids* 139:108496

[17] Chen Z, Ma J, Li P, Wen B, Wang Y, et al. 2023. Preparation of hypoglycemic anthocyanins from mulberry (*Fructus mori*) fruits by ultrahigh pressure extraction. *Innovative Food Science & Emerging Technologies* 84:103255

[18] Lv Y, Yue H, Tan C, Liao H. 2025. Characterization of a novel biodegradable active film with rose polyphenol extract and its application in edible oil packaging. *Food Bioscience* 63:105784

[19] Zhu Y, Zheng X, Zeng Q, Zhong R, Guo Y, et al. 2023. The inhibitory effect of large yellow croaker roe phospholipid as a potential antioxidant on fish oil oxidation stability. *Food Bioscience* 56:103291

[20] Wang H, Chen X, Yang H, Wu K, Guo M, et al. 2025. A novel gelatin composite film with melt extrusion for walnut oil packaging. *Food Chemistry* 462:141021

[21] Ahmadi N, Ghavami M, Rashidi L, Gharachorloo M, Nateghi L. 2024. Effects of adding green tea extract on the oxidative stability and shelf life of sunflower oil during storage. *Food Chemistry: X* 21:101168

[22] Liu S, Zhang Y. 2024. Antioxidant properties and electrochemical activity of anthocyanins and anthocyanidins in mulberries. *Journal of Food Measurement and Characterization* 18:3569–3576

[23] Zeng P, Chen X, Qin YR, Zhang YH, Wang XP, et al. 2019. Preparation and characterization of a novel colorimetric indicator film based on gelatin/polyvinyl alcohol incorporating mulberry anthocyanin extracts for monitoring fish freshness. *Food Research International* 126:108604

[24] Ma Q, Wang L. 2016. Preparation of a visual pH-sensing film based on tara gum incorporating cellulose and extracts from grape skins. *Sensors and Actuators B: Chemical* 235:401–407

[25] Gao L, Sun H, Nagassa M, Li X, Pei H, et al. 2024. Edible film preparation by anthocyanin extract addition into acetylated cassava starch/sodium carboxymethyl cellulose matrix for oxidation inhibition of pumpkin seeds. *International Journal of Biological Macromolecules* 267:131439

[26] Gasti T, Dixit S, D'Souza OJ, Hiremani VD, Vootla SK, et al. 2021. Smart biodegradable films based on chitosan/methylcellulose containing *Phyllanthus reticulatus* anthocyanin for monitoring the freshness of fish fillet. *International Journal of Biological Macromolecules* 187:451–461

[27] Qin Y, Xu F, Yuan L, Hu H, Yao X, et al. 2020. Comparison of the physical and functional properties of starch/polyvinyl alcohol films containing anthocyanins and/or betacyanins. *International Journal of Biological Macromolecules* 163:898–909

[28] Kang S, Wang H, Xia L, Chen M, Li L, et al. 2020. Colorimetric film based on polyvinyl alcohol/okra mucilage polysaccharide incorporated with rose anthocyanins for shrimp freshness monitoring. *Carbohydrate Polymers* 229:115402

[29] Liu X, Chen L, Dong Q, Wang Z, Zhang D, et al. 2022. Emerging starch composite nanofibrous films for food packaging: facile construction, hydrophobic property, and antibacterial activity enhancement. *International Journal of Biological Macromolecules* 222:868–879

[30] Ding F, Wu R, Huang X, Shi J, Zou X. 2024. Anthocyanin loaded composite gelatin films crosslinked with oxidized alginate for monitoring spoilage of flesh foods. *Food Packaging and Shelf Life* 42:101255

[31] Zhao H, Liu W, Min C, Qi Y, Chen X, et al. 2025. pH-responsive color indicator film based on gelatin/chitosan cross-linking with anthocyanin-Fe^{2+} chelate for pork freshness monitoring. *Food Hydrocolloids* 162:110895

[32] Xu M, Fang D, Shi C, Xia S, Wang J, et al. 2025. Anthocyanin-loaded polylactic acid/quaternized chitosan electrospun nanofiber as an intelligent and active packaging film in blueberry preservation. *Food Hydrocolloids* 158:110586

[33] Li R, Feng H, Wang S, Zhuang D, Zhu J. 2024. A colorimetry-enhanced tri-functional film with high stability by polyphenol-anthocyanin co-pigmentation/conjugate: new prospect for active intelligent food packaging. *Food Chemistry* 447:138927

[34] Wu C, Li Y, Sun J, Lu Y, Tong C, et al. 2020. Novel konjac glucomannan films with oxidized chitin nanocrystals immobilized red cabbage anthocyanins for intelligent food packaging. *Food Hydrocolloids* 98:105245

[35] Qi Y, Li Y, Cui J. 2024. Rapid-response nanofiber films against ammonia based on black wolfberry anthocyanins, polyvinyl alcohol and sodium alginate for intelligent packaging. *International Journal of Biological Macromolecules* 279:135390

[36] Li J, Zhang X, Zhou W, Tu Z, Yang S, et al. 2023. Intelligent films based on highland barley β-glucan/highland barley prolamin incorporated with black rice bran anthocyanins. *Food Packaging and Shelf Life* 39:101146

[37] Cao J, Wang C, Zou Y, Xu Y, Wang S, et al. 2023. Colorimetric and antioxidant films based on biodegradable polymers and black nightshade (*Solanum nigrum* L.) extract for visually monitoring *Cyclina sinensis* freshness. *Food Chemistry: X* 18:100661

[38] Tao X, Chen C, Li Y, Qin X, Zhang H, et al. 2023. Improving the antioxidant activity, *in vitro* digestibility and reducing the allergenicity of whey protein isolate by glycosylation with short-chain inulin and interaction with cyanidin-3-glucoside. *Food Hydrocolloids* 139:108586

[39] Alizadeh-Sani M, Tavassoli M, McClements DJ, Hamishehkar H. 2021. Multifunctional halochromic packaging materials: saffron petal anthocyanin loaded-chitosan nanofiber/methyl cellulose matrices. *Food Hydrocolloids* 111:106237

[40] Mareček V, Mikyška A, Hampel D, Čejka P, Neuwirthová J, et al. 2017. ABTS and DPPH methods as a tool for studying antioxidant capacity of spring barley and malt. *Journal of Cereal Science* 73:40–45

[41] Huang X, Luo X, Liu L, Dong K, Yang R, et al. 2020. Formation mechanism of egg white protein/κ-Carrageenan composite film and its application to oil packaging. *Food Hydrocolloids* 105:105780

[42] Luo SZ, Chen SS, Pan LH, Qin XS, Zheng Z, et al. 2017. Antioxidative capacity of crude camellia seed oil: impact of lipophilization products of blueberry anthocyanin. *International Journal of Food Properties* 20:1627–1636

Copyright: © 2026 by the author(s). Published by Maximum Academic Press on behalf of China Agricultural University, Zhejiang University and Shenyang Agricultural University. This article is an open access article distributed under Creative Commons Attribution License (CC BY 4.0), visit https://creativecommons.org/licenses/by/4.0/.